Photochemical & Photobiological Sciences

Accepted Manuscript

This is an *Accepted Manuscript*, which has been through the Royal Society of Chemistry peer review process and has been accepted for publication.

Accepted Manuscripts are published online shortly after acceptance, before technical editing, formatting and proof reading. Using this free service, authors can make their results available to the community, in citable form, before we publish the edited article. We will replace this *Accepted Manuscript* with the edited and formatted *Advance Article* as soon as it is available.

You can find more information about *Accepted Manuscripts* in the Information for Authors.

Please note that technical editing may introduce minor changes to the text and/or graphics, which may alter content. The journal's standard Terms & Conditions and the Ethical guidelines still apply. In no event shall the Royal Society of Chemistry be held responsible for any errors or omissions in this *Accepted Manuscript* or any consequences arising from the use of any information it contains.

ROYAL SOCIETY OF CHEMISTRY

www.rsc.org/pps

Effects of organic acids and initial solution pH on photocatalytic degradation of bisphenol A (BPA) in a photo-Fenton-like process using Goethite (α-FeOOH)

Guangshan Zhang,[a] Qiao Wang,[a] Wen Zhang,[b] Tian Li,[a] Yixing Yuan[a] and Peng Wang*[a]

[a]*State Key Laboratory of Urban Water Resource and Environment, School of Municipal* and *Environmental Engineering, Harbin Institute of Technology, Harbin 150090, PR China*

[b]*John A. Reif, Jr. Department of Civil & Environmental Engineering, New Jersey Institute of Technology, Newark, NJ 07102, USA*

*Corresponding author. Address: No. 73 Huanghe Road, Nangang District, Harbin 150090, China. Tel./fax: +86-451-86283557.

E-mail address: pwang73@vip.sina.com (Peng Wang)

Abstract:

This work investigated the effects of organic acids and initial solution pH on the photodegradation of BPA in a photo-Fenton-like process using α-FeOOH as a catalyst. The results showed that the additions of different organic acids affected the formation of the ferric-carboxylate complexes and free radicals, which in turn varied the photodegradation efficacy. Compared with the other acids, oxalic acid (OA) was found to be the most effective in enhancing the photodegradation of BPA, which strongly depends on the OA concentration. Particularly, the addition of OA could significantly extend the working pH from acidic to neutral ranges in the photocatalytic process and thus the acidification pretreatment may not be needed. The high photocatalytic degradation of BPA occurred at pH 6.0, due to the formation of ferric-oxalate complexes and •OH radicals in the synergistic interactions of OA and α-FeOOH. The finding highlights that the oxalate-promoted photo-Fenton-like process using α-FeOOH catalyst may be used for wastewater treatment without pH adjustment.

Keywords: α-FeOOH; BPA; pH; Oxalic acid; Photodegradation

1. Introduction

The environmental release of BPA from urban sewage and factories are accelerated with rapid economic development in recent years.[1,2] BPA has been applied in the production of epoxy resins, polycarbonate plastics, flame retardants and other chemical products.[3,4] Over the last decade, BPA has been detected in environmental waters, humans and wildlife, even in the remote polar areas.[5-7] As an endocrine disrupting compound, BPA is harmful to the environment and human health even at a low-dose exposure.[3,8] Thus, BPA presents serious environmental and health concerns after entering water or wastewater systems.

The advanced oxidation processes (AOPs) have been developed as effective technologies in the removal of various recalcitrant organic pollutants.[9,10] Compared with biodegradation and adsorption, AOPs are capable of destroying trace level organic pollutants by free radicals (mainly hydroxyl radicals or •OH).[11-14] As one of the popular AOPs, the photo-Fenton process is based on the following photochemical reactions:[15,16]

$$Fe^{2+} + H_2O_2 \rightarrow Fe^{3+} + \bullet OH + \bullet OH^- \quad (1)$$

$$FeOH^{2+} + h\nu \rightarrow Fe^{2+} + \bullet OH \quad (2)$$

The complex $FeOH^{2+}$ is the dominant Fe^{3+} species in solution at pH 2-3, which can produce •OH and regenerate Fe^{2+} to react with more H_2O_2.[17-19] Furthermore, •OH in acidic medium can efficiently degrade organic pollutants. Unfortunately, homogeneous photo-Fenton processes have three critical disadvantages that limit their practical applications, including: (1) the need to continuously supply ferrous salt into the reaction system; (2) accumulation of iron sludge,[20] which results in the secondary pollution and costly separation; and (3) the narrow working pH range (2.5-3.5),[21] which requires acidification.

To overcome the above drawbacks in the conventional photo-Fenton process, heterogeneous photo-Fenton-like processes have been developed with innovative

photocatalysts, such as α-FeOOH,[17,22] β-FeOOH,[14,23] Fe_2O_3,[11,24] $BiFeO_3$,[25-27] and $Fe_2(MoO_4)_3$.[28] These catalysts commonly contain iron elements that can activate H_2O_2 to degrade a wide spectrum of organic pollutants, and thus enhance the wastewater treatment efficiency.[16,28] Among these catalysts, α-FeOOH shows excellent photocatalytic performances in the removal of organic pollutants owing to its stable chemical properties, large specific surface area[29,30] and unique particulate structures.[31] The photodegradation efficiency of organic pollutants is usually influenced by the synthesis method of catalysts, initial solution pH, H_2O_2 dosage, light intensity, and organic acid addition.[18,22,32,33] The narrow pH range is one of the major hurdles for practical applications in wastewater treatment. One of the remedial methods is to spike organic acids into the water to broaden the working pH range of the α-FeOOH/H_2O_2 photocatalysis. Furthermore, the complexes formed by iron and organic acids, e.g., ferric-oxalate, could catalyze the production of •OH radicals and prevent iron precipitation even at neutral pHs.[17,18] However, to the best of our knowledge, there have been few studies that systematically investigated the effects of addition of different organic acids and the initial solution pHs on a photo-Fenton-like photodegradation process in wastewater treatment.

In this work, the α-FeOOH catalyst was prepared for the photo-Fenton-like process to evaluate the degradation efficiency of BPA. The photocatalytic activities of the α-FeOOH/H_2O_2 photocatalysis were first evaluated with additions of various organic acids. Moreover, the roles of the initial solution pH in the BPA removal were analyzed. The photodegradation mechanism in the heterogeneous photo-Fenton-like reaction in the presence of oxalic acid was proposed.

2. Experimental

2.1. Materials

BPA ($C_{15}H_{16}O_2$) was purchased from Tianjin Kermel Chemical Reagent Co., Ltd.,

China. Hydrogen peroxide (30%, w/w) and $Fe(NO_3)_3 \cdot 9H_2O$ were purchased from Sinopharm Chemical Reagent Co., Ltd., China. The other chemicals used in the experiments were purchased from Aladdin Reagent Co., Ltd. They were all of analytical grade and used without further purification. All solutions were prepared using deionized (DI) water at room temperature.

2.2. Synthesis of the α-FeOOH catalyst

The α-FeOOH catalysts were synthesized by the precipitation method.[2,34] Briefly, 250 mL of a 0.5 $mol \cdot L^{-1}$ $Fe(NO_3)$ solution was slowly titrated with a 2.5 $mol \cdot L^{-1}$ NaOH solution at a constant rate of 5 $mL \cdot min^{-1}$ with continuously magnetic stirring at a speed of 300 rpm. NaOH was added dropwise until the reaction solution reached a pH of 12. Then the suspension was placed in a drying oven at 60 ℃ for 12 h, and cooled at room temperature. The precipitate was centrifuged and washed repeatedly with DI water. Finally, the obtained solid was vacuum dried at 60 ℃ for 2 h.

2.3. Characterization of the α-FeOOH catalyst

The crystallinity of the catalysts was determined by X-ray diffraction (XRD) which was equipped with a diffractometer (X'Pert PROThermo, PANalytical, Holland) using a Cu Kα radiation source under a voltage of 40 kV and current of 200 mA. The XRD patterns were recorded with a scanning rate of $6° \cdot min^{-1}$ from 10° to 80°. The morphology of the goethite was observed by scanning electron microscope-energy dispersive X-ray spectroscopy (SEM/EDX; FEI QUANTA 200). The sample powders were spread on a carbon-coated sample mount and coated with gold to prevent surface charging effects. The particle zeta potential was determined using dynamic light scattering (DLS) on a Zetasizer Nano ZS instrument (Malvern, ZEN3600). The temperature was maintained at 25 ℃, and the scattering angle was 173° from the incident laser beam.[35] The determination of hydroxyl radicals was conducted using a FP-6500 fluorescence spectrophotometer (Jasco, Japan). The capture agent was

terephthalic acid (800 $mg \cdot L^{-1}$). The generated hydroxyl product (namely 2-hydroxyterephthalic acid) has a fluorescence emission peak at 425 nm under the excitation wavelength at 315 nm.[36]

2.4. Photocatalytic experiments

The photocatalytic experiments were conducted in a cylindrical reactor (BL-GHX-II, Xian Bilon Biological Technology Co., Ltd., China). **Fig. S1** in the supporting information (SI) shows the major components of the photocatalytic reactor. The photoreactor was placed 5 cm away from a 100 W high-pressure mercury lamp with a primary wavelength (365 nm). The irradiation intensity was about 3.4 $W \cdot cm^{-2}$, measured by a spectroradiometer. A quartz tube with water recirculation was used for cooling at room temperature (20 °C). In the experiment, a photocatalyst suspension was prepared by dispersing 0.15 g of the α-FeOOH catalyst and a certain amount of an organic acid in a 300 mL BPA aqueous solution (10 $mg \cdot L^{-1}$). The acids to be spiked into the suspension included oxalic acid (OA), acetic acid (AA), citric acid (CA), malic acid (MA), and tartaric acidoxalic (TA). These organic acids were chosen because of their cheap cost, safety, and wide industrial applications. In the experiments, the initial solution pH was maintained at 6.0 (without pH control) and the final concentrations of these acids in the solution were all 30 $mg \cdot L^{-1}$. The solution pH was adjusted with 0.1 M HCl or 0.1 M NaOH, and then the suspension was magnetically stirred in the dark for 30 min to ensure the adsorption equilibrium of BPA on the catalysts. Before irradiation, H_2O_2 was added to the reaction solution at a final concentration of 50 $mg \cdot L^{-1}$. Liquid samples were taken out from the solution after different irradiation time and immediately filtered through 0.22-μm hydrophilic polyethersulfone membranes (Pall Life Sciences, Inc.).

The BPA concentration was analyzed using a high performance liquid chromatography (HPLC) (LC-20AD; Shimadzu) equipped with an electrolytic conductivity detector (CDD-10AVP; Shimadzu). Mobile phase A was methanol while

phase B was the DI water containing 20 mmol·L^{-1} of KH_2PO_4, and the flow rate was 0.8 mL·min^{-1}. The limit of detection for BPA is 0.01 mg·L^{-1}. All measurements of the BPA degradation at different irradiation times were performed three times to confirm their reproducibility. The presented data points were mean values with standard deviations as error bars. The removal efficiency of BPA was calculated as follows:

$$R = \frac{C_0 - C}{C_0} \times 100\% \quad (3)$$

where R, C_0 and C were the removal efficiency of BPA, the initial concentration and the concentration of BPA after irradiation at various time interval (t), respectively.

3. Results and discussion

3.1. Characterization

Fig. 1a displays the XRD pattern of the catalyst. Three major peaks are clearly observed at 2θ values of 21.28°, 33.28° and 36.74°, which are similar to the pure goethite pattern reported in the XRD standard data base library (JCPDS 29-0713), indicating that the sample is phase-pure α-FeOOH crystal with good crystallinity. The morphology of the α-FeOOH catalyst was characterized by SEM (**Fig. 1b**). The α-FeOOH particles have a uniformly rod-like structure. The length of particle is approximately 400-500 nm and the width is about 25-50 nm. The BET surface area was found to be 41.3 $m^2 \cdot g^{-1}$, which is consistent with previously reported.[30]

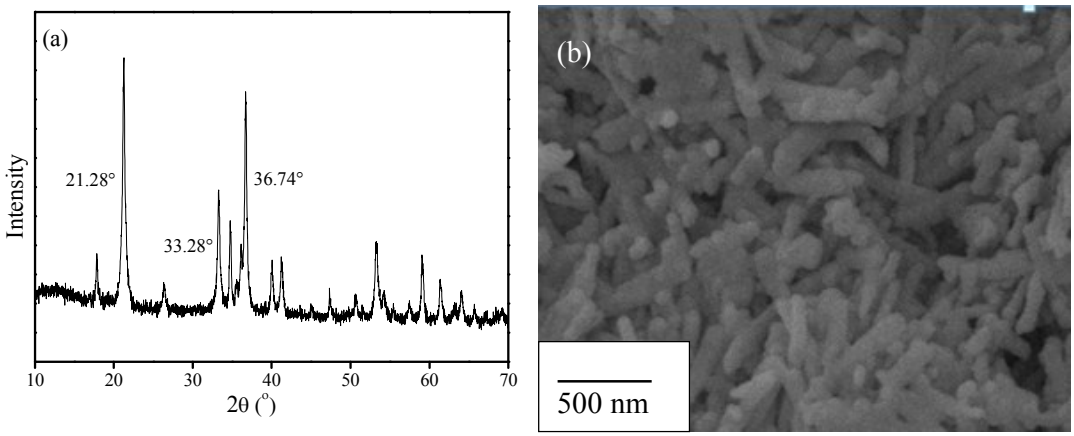

Fig. 1 (a) XRD pattern and (b) SEM image of goethite catalyst.

3.2. The influences of additions of various organic acids in the photo-Fenton-like process

3.2.1. Comparison of different organic acids

Fig. 2 shows that the removal rate of BPA is about 64.5% in the α-FeOOH/H_2O_2 system without addition of organic acids. However, the removal rates of BPA became 96.4%, 43.2%, 34.5%, 42.4%, and 49.2% in the presence of OA, AA, CA, MA and TA, respectively. Interestingly, only the introduction of OA enhanced the photodegradation in the α-FeOOH/H_2O_2 system, whereas AA, CA, MA, and TA inhibited the photodegradation. The different effects of organic acids on photodegradation of BPA may be caused by several plausible reasons, including the surface reactions between catalysts and organic acids, acid dissociation, and photochemical interactions of organic acids with radicals and absorbance of organic acids toward UV, which are discussed later.

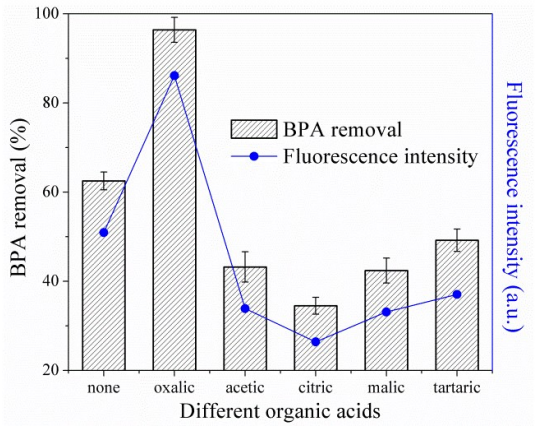

Fig. 2 BPA removal ratios and corresponding amount of •OH generated by the α-FeOOH/H_2O_2 photocatalysis in the presence of various organic acids. Reaction conditions: BPA aqueous solution (10 mg·L^{-1}) 300 mL; initial solution pH 6.0; photocatalyst 0.15 g; H_2O_2 concentration 50 mg·L^{-1}; concentration of OA, AA, CA, MA and TA , 30 mg·L^{-1} respectively; reaction time 120 min.

To determine how the presence of organic acids in the α-FeOOH/H_2O_2 system varied the •OH production, the relative fluorescence intensities of the generated 2-hydroxyterephthalic acid are monitored and shown in **Fig. 2**. After adding the various organic acids, the •OH production followed the order of: OA > TA > AA > MA > CA. Only OA could enhance the •OH production in the α-FeOOH/H_2O_2 system, probably because OA can form the ferric-oxalate complexes with α-FeOOH, which generated active species and transformed Fe^{2+} to Fe^{3+}, resulting in a better formation of Fenton reagent •OH than the H_2O_2 alone. Obviously, the •OH production strongly depends on the acidity or dissociation potential of organic acids.[37,38] TA, AA, MA, and CA are found to inhibit the BPA photodegradation, probably because they can quench and reduce available •OH for BPA degradation.

3.2.2. Effect of oxalic acid concentration on the photodegradation of BPA

To determine the optimal concentration of oxalic acid for the photodegradation of BPA in the α-FeOOH/H_2O_2/oxalate system, a set of experiments with different concentrations of oxalic acid in the range of 0-50 mg·L^{-1} without pH control (pH =

6.0) were carried out under UV irradiation. **Fig. 3** shows that the BPA removal rate increases slightly after the addition of 10 $mg \cdot L^{-1}$ oxalic acid. The removal rate reached the maximum (96.4%) when the concentration of oxalic acid was 30 $mg \cdot L^{-1}$, which is about 30% increase compared to the result without oxalic acid. The removal rates of 81% and 78% were observed at an initial concentration of 40 $mg \cdot L^{-1}$ and 50 $mg \cdot L^{-1}$ respectively. The low concentrations (10-30 $mg \cdot L^{-1}$) of OA increased the removal of BPA, as OA could be readily transformed into catalytically active Fe^{3+}-oxalate complex and promoted the photocatalytic oxidation reaction. On the contrary, at high concentrations OA inhibited the degradation, because excessive OA may compete the adsorption sites on the surface of the α-FeOOH and quench •OH radicals and depressed the formation of H_2O_2. Thus, the BPA photodegradation was decreased, which is consistent with previous studies.[18,39]

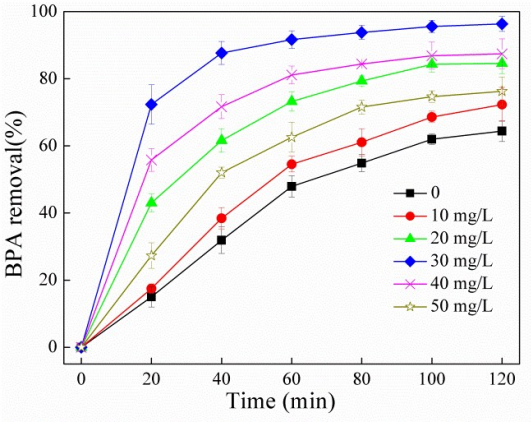

Fig. 3 BPA removal rate at different OA concentrations. Reaction conditions: BPA aqueous solution (10 $mg \cdot L^{-1}$) 300 mL; initial solution pH 6.0; photocatalyst 0.15 g; H_2O_2 concentration 50 $mg \cdot L^{-1}$.

3.3. Performance of the initial solution pH on the BPA degradation

Fig. 4a compares the degradation of BPA in the presence of OA at different initial solution pH values. Controlled experiments (without OA) were conducted under other identical conditions (**Fig. 4b**). **Fig. 4** indicates that the photodegradation of BPA depends strongly on the initial solution pH. The BPA removal rate reached maximum

(96.4%) at pH 6.0 with a pseudo-second order rate constant of 0.0207 $L \cdot mg^{-1} \cdot min^{-1}$. However, in pH from 6.0 to 9.0, the photocatalytic activity decreased appreciably with or without the presence of OA.

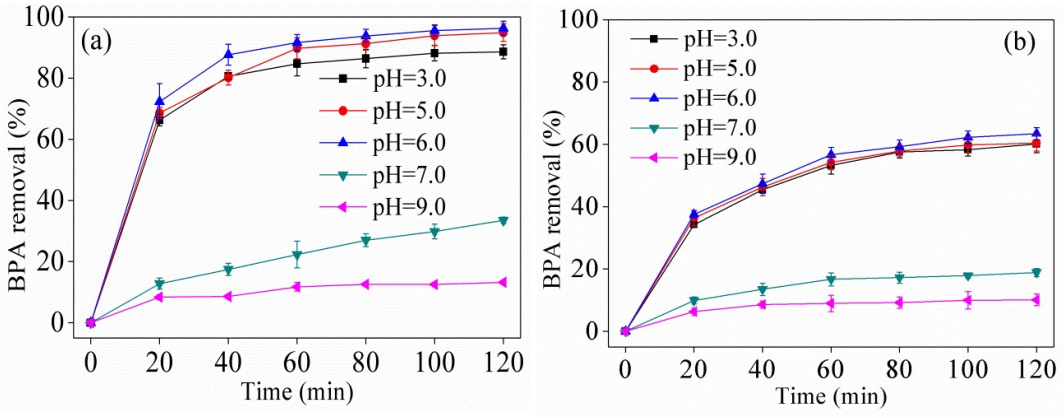

Fig. 4 BPA photodegradation at the different initial solution pH values by (a) α-FeOOH/H_2O_2 photocatalysis in the presence of OA (30 $mg \cdot L^{-1}$) and (b) α-FeOOH/H_2O_2 photocatalysis without OA. Reaction conditions: BPA aqueous solution (10 $mg \cdot L^{-1}$) 300 mL; photocatalyst 0.15 g; H_2O_2 concentration 50 $mg \cdot L^{-1}$.

The reaction rate constants at different pH values are calculated and shown in **Fig. 5a.** The BPA photodegradation under different pH conditions was fitted with pseudo-second order kinetics. The rate constant increased as the pH increased from 3.0-6.0; whereas, it decreased remarkably from 6.0-9.0. Moreover, the rate constant at pH 6.0 is 0.0207 $L \cdot mg^{-1} \cdot min^{-1}$, which is 130 times higher than that at pH 9.0. **Fig. 5b** shows the zeta potential of the α-FeOOH catalysts at the different solution pH values. The isoelectric point of α-FeOOH is determined to be 6.2, similar to literature values.[40,41] Therefore, the photocatalyst particle surface carries a positive charge (≡Fe(III)OH_2^+) in the reaction solution pH of below 6.2, which electrostatically attracts negatively charged oxalate. On the contrary, the α-FeOOH surface contains the negative ions of FeO^- in neutral and alkaline solutions, which could slow down the interactions between BPA and α-FeOOH catalyst. Furthermore, the influence of the solution pH on the formation of •OH was assessed by the relative fluorescence

intensities of the generated 2-hydroxyterephthalic acid in the α-FeOOH/H_2O_2/oxalate system (**Fig. 6**). The peak of •OH generation occurred at pH 6, which coincided with the result of BPA photodegradation (**Fig. 4a**). Clearly, the blending of OA with α-FeOOH enhances the amount of •OH radicals and extends the reaction pH to near neutral for the practical applications of BPA degradation in wastewater.

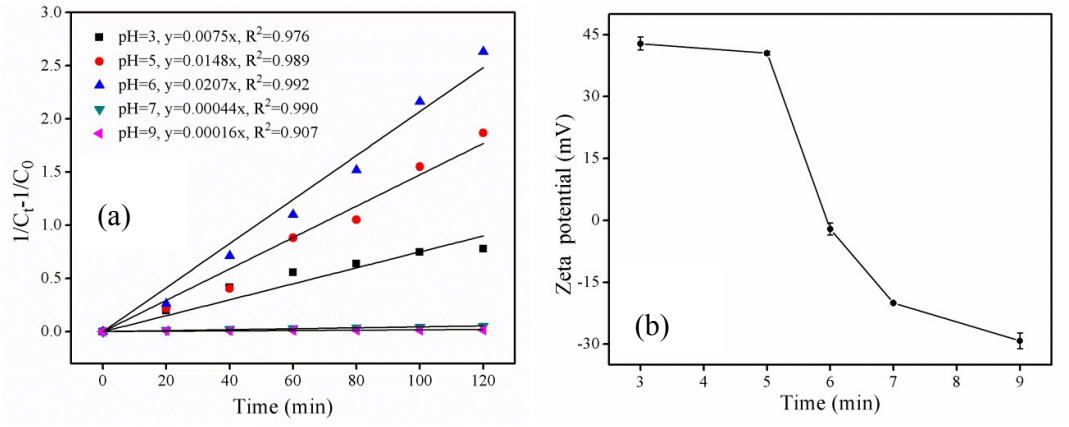

Fig. 5 (a) Plot of ($1/C_t$-$1/C_0$) as a function of irradiation time for photocatalysis of BPA solution (Reaction conditions: BPA aqueous solution (10 mg·L^{-1}) 300 mL; photocatalyst 0.15 g; H_2O_2 concentration 50 mg·L^{-1}; OA concentration 30 mg·L^{-1}), and (b) the zeta potential of the α-FeOOH catalysts in water at different pH values.

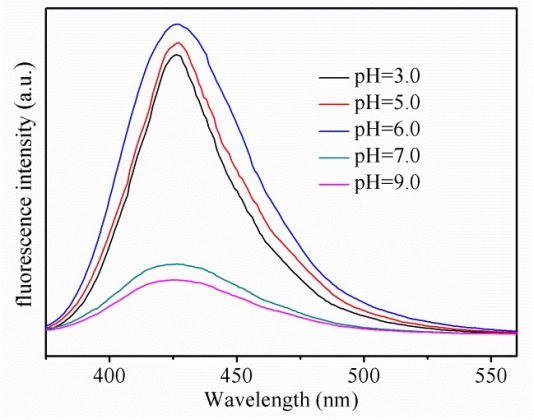

Fig. 6 Comparison of •OH generated in α-FeOOH/H_2O_2 photocatalysis in the presence of oxalic acid. Reaction conditions: BPA aqueous solution (10 mg·L^{-1}) 300 mL; photocatalyst 0.15 g; H_2O_2 concentration 50 mg·L^{-1}; OA concentration 30 mg·L^{-1}.

3.4. Mechanism of the Goethite/oxalate photodegradation process

These organic acids, once spiked into the solution, should dissociate into protons and its conjugate base to different extent because of their different dissociation equilibrium.[42] **Fig. S2** shows that OA would substantially decrease the solution pH after equilibrium among the selected organic acids due to its high dissociation constants (pk_{a1} = 1.27 and pk_{a2} = 4.27). However, the solution pH after addition of different organic acids was not observed to drop as predicted, probably because the surface reactions between organic acids and α-FeOOH (See below) could provide certain buffering capacity for the solution pH. Clearly, the reaction between OA and α-FeOOH might proceed more completely due to the highest dissociation constants of OA compared with those of other organic acids (e.g., $pK_a > 3$).

OA: $2\alpha\text{-FeOOH} + H_2C_2O_4 \rightarrow [\equiv Fe(III)(C_2O_4)]^+ + 2H_2O$ (4)

AA: $\alpha\text{-FeOOH} + H_4C_2O_2 \rightarrow [\equiv Fe(III)O(H_3C_2O_2)]^+ + H_2O$ (5)

CA: $3\alpha\text{-FeOOH} + C_6H_8O_7 \rightarrow [\equiv Fe(III)O(H_5C_6O_7)]^+ + 3H_2O$ (6)

MA: $2\alpha\text{-FeOOH} + C_4H_6O_5 \rightarrow [\equiv Fe(III)O(H_4C_4O_5)]^+ + 2H_2O$ (7)

TA: $2\alpha\text{-FeOOH} + C_4H_6O_6 \rightarrow [\equiv Fe(III)O(H_4C_4O_6)]^+ + 2H_2O$ (8)

It is worth noting that the conjugated complex or Fe^{3+}-oxalate complex between α-FeOOH and OA may have the minimum level of hydrogen atoms, which may result in different photochemical properties (e.g., UV absorbance) and formation of radicals. As **Fig. 2** shows, the BPA degradation is highly linked with the radical formation. Unlike OA, other organic acids (especially CA) are efficient radical quenchers and thus could reduce the availability of •OH radicals.[43] Similar to the α-FeOOH/H_2O_2/iso-propyl alcohol system,[22] the photochemical reactions for OA and α-FeOOH may create heterogeneous photo-Fenton-like processes as follows:[4,44,45]

$[\equiv Fe(III)(C_2O_4)]^+ + h\nu \rightarrow [\equiv Fe(II)(C_2O_4)\bullet^-]$ (9)

$[\equiv Fe(II)(C_2O_4)\bullet^-] \rightarrow \equiv Fe(II)O + CO_2 + CO_2\bullet^-$ (10)

$CO_2\bullet^- + O_2 \rightarrow + CO_2 + O_2\bullet^-$ (11)

$O_2\bullet^- + H^+ \rightarrow + \bullet OOH$ (12)

$O_2\bullet^-/\bullet OOH + H^+ + Fe^{2+} \rightarrow + Fe^{3+} + H_2O_2$ (13)

$O_2\bullet^-/\bullet OOH + Fe^{3+} \rightarrow + Fe^{2+} + O_2$ (14)

$Fe^{3+} + H_2O_2 \rightarrow Fe^{3+} + OH^- + \bullet OH$ (15)

$BPA + \bullet OH \rightarrow\rightarrow\cdots\cdots\rightarrow CO_2 + H_2O$ (16)

Under UV-light irradiation, Fe^{3+} in the Fe^{3+}-oxalate complex is reduced into Fe^{2+}. Then, the Fe^{2+}-oxalate complex reacts with O_2 and generate reactive oxygen species (e.g., $O_2\bullet^-$ and •OOH). The concomitant reaction between Fe^{2+} and H_2O_2 leads to the regeneration Fe^{3+} and the production of •OH. Therefore, the addition of OA promoted the photodegradation of BPA and effectively extended the working solution pH to near neutral, which is important for practical wastewater treatment.

4. Conclusions

The photodegradation of BPA in the heterogeneous photo-Fenton-like system with α-FeOOH was found to vary with the addition of organic acids and solution pH. The addition of various organic acids influenced the BPA removal efficiency in the α-FeOOH/H_2O_2 system owing to the formation of ferric-carboxylate complexes and the •OH formation. At low concentrations (<30 $mg \cdot L^{-1}$), oxalic acid enhanced the photodegradation of BPA and the formation of •OH in α-FeOOH/H_2O_2 system among organic acids. The highest removal rate (96.4%) in the α-FeOOH/H_2O_2/oxalate system was obtained at pH 6.0, which highlights the potential of the photo-Fenton-like processes in practical wastewater treatment applications.

Acknowledgments

This work was supported by Open Project of State Key Laboratory of Urban Water Resource and Environment, Harbin Institute of Technology (No. QA201610-01) and National Science Foundation for Postdoctoral Scientists of China (No. 2014M561356).

References

1 Y. Baba, T. Yatagai, T. Harada, Y. Kawase, Hydroxyl radical generation in the photo-Fenton process: Effects of carboxylic acids on iron redox cycling, *Chem. Eng. J.*, 2015, 277: 229-241

2 G. Zhao, Q. Y. Huang, X. M. Rong, P. Cai, W. Liang, K. Dai, Biodegradation of methyl parathion in the presence of goethite: The effect of Pseudomonas sp. Z1 adhesion, *Int. Biodeterior. Biodegrad.*, 2014, 86: 294-299

3 J. I. Nieto-Juarez, T. Kohn, Virus removal and inactivation by iron (hydr)oxide-mediated Fenton-like processes under sunlight and in the dark, *Photochem. Photobiol. Sci.*, 2013, 12(9): 1596-1605

4 S. Q. Liu, L. R. Feng, N. Xu, Z. G. Chen, X. M. Wang, Magnetic nickel ferrite as a heterogeneous photo-Fenton catalyst for the degradation of rhodamine B in the presence of oxalic acid, *Chem. Eng. J.*, 2012, 203: 432-439

5 X. T. Guo, C. Yang, Z. Dang, Q. Zhang, Y. J. Li, Q. Y. Meng, Sorption thermodynamics and kinetics properties of tylosin and sulfamethazine on goethite, *Chem. Eng. J.*, 2013, 223: 59-67

6 S. L. Wang, C. Y. Wang, C. Y. Liu, M. Zhang, H. Ma, J. Li, Fabrication of superhydrophobic spherical-like alpha-FeOOH films on the wood surface by a hydrothermal method, *Colloid Surf. A-Physicochem. Eng. Asp.*, 2012, 403: 29-34

7 J. M. Monteagudo, A. Durán, M. Aguirre, I. S. Martín, Photodegradation of Reactive Blue 4 solutions under ferrioxalate-assisted UV/solar photo-Fenton system with continuous addition of H_2O_2 and air injection, *Chem. Eng. J.*, 2010, 162(2): 702-709

8 H. Li, R. Priambodo, Y. Wang, H. Zhang, Y.-H. Huang, Mineralization of bisphenol A by photo-Fenton-like process using a waste iron oxide catalyst in a three-phase fluidized bed reactor, *J. Taiwan Inst. Chem. Eng.*, 2015, 53: 68-73

9 S. H. Tian, J. L. Zhang, J. Chen, L. J. Kong, J. Lu, F. C. Ding, Y. Xiong, $Fe_2(MoO_4)_3$ as an Effective Photo-Fenton-like Catalyst for the Degradation of Anionic and Cationic Dyes in a Wide pH Range, *Ind. Eng. Chem. Res.*, 2013, 52(37): 13333-13341

10 H. Y. He, J. Fei, J. Lu, High photocatalytic and photo-Fenton-like activities of ZnO-reduced graphene oxide nanocomposites in the degradation of malachite green in water, *Micro & Nano Letters*, 2015, 10(8): 389-394

11 C. R. Jiang, Z. C. Xu, Q. W. Guo, Q. F. Zhuo, Degradation of bisphenol A in water by the heterogeneous photo-Fenton, *Environ. Technol.*, 2014, 35(8): 966-972

12 C. A. Staples, P. B. Dorn, G. M. Klecka, S. T. O'Block, L. R. Harris, A review of the environmental fate, effects, and exposures of bisphenol A, *Chemosphere*, 1998, 36(10): 2149-2173

13 S. Fassi, K. Djebbar, I. Bousnoubra, H. Chenini, T. Sehili, Oxidation of bromocresol green by different advanced oxidation processes: Fenton, Fenton-like, photo-Fenton, photo-Fenton-like and solar light. Comparative study, *Desalin. Water Treat.*, 2014, 52(25-27): 4982-4989

14 J. M. Song, H. Wang, G. Hu, S. J. Zhao, H. Q. Hu, B. K. Jin, $ZnWO_4$–Cu system with enhanced photocatalytic activity by photo-Fenton-like synergistic reaction, *Mater. Res. Bull.*, 2012, 47(11): 3296-3300

15 M. Tokumura, M. Shibusawa, Y. Kawase, Dynamic simulation of degradation of toluene in waste gas by the photo-Fenton reaction in a bubble column, *Chem. Eng. Sci.*, 2013, 100: 212-224

16 N. H. M. Azmi, O. B. Ayodele, V. M. Vadivelu, M. Asif, B. H. Hameed, Fe-modified local clay as effective and reusable heterogeneous photo-Fenton catalyst for the decolorization of Acid Green 25, *J. Taiwan Inst. Chem. Eng.*, 2014, 45(4): 1459-1467

17 Y. Mameri, N. Debbache, M. e. m. Benacherine, N. Seraghni, T. Sehili, Heterogeneous photodegradation of paracetamol using Goethite/H_2O_2 and Goethite/oxalic acid systems under artificial and natural light, *J. Photochem. Photobiol. A-Chem.*, 2016, 315: 129-137

18 L. I. Doumic, P. A. Soares, M. A. Ayude, M. Cassanello, R. A. R. Boaventura, V. J. P. Vilar, Enhancement of a solar photo-Fenton reaction by using ferrioxalate complexes for the treatment of a synthetic cotton-textile dyeing wastewater, *Chem. Eng. J.*, 2015, 277: 86-96

19 C. Catastini, M. Sarakha, G. Mailhot, M. Bolte, Iron (III) aquacomplexes as effective photocatalysts for the degradation of pesticides in homogeneous aqueous solutions, *Sci. Total Environ.*, 2002, 298(1-3): 219-228

20 P. Bautista, A. F. Mohedano, J. A. Casas, J. A. Zazo, J. J. Rodriguez, An overview of the application of Fenton oxidation to industrial wastewaters treatment, *J. Chem. Technol. Biotechnol.*, 2008, 83(10): 1323-1338

21 G. K. Zhang, Y. Y. Gao, Y. L. Zhang, Y. D. Guo, Fe_2O_3-Pillared Rectorite as an Efficient and Stable Fenton-Like Heterogeneous Catalyst for Photodegradation of Organic Contaminants, *Environ. Sci. Technol.*, 2010, 44(16): 6384-6389

22 J. Sharma, I. M. Mishra, V. Kumar, Mechanistic study of photo-oxidation of Bisphenol-A (BPA) with hydrogen peroxide (H_2O_2) and sodium persulfate (SPS), *J. Environ. Manage.*, 2016, 166: 12-22

23 Y. P. Zhao, J. Y. Hu, H. B. Chen, Elimination of estrogen and its estrogenicity by heterogeneous photo-Fenton catalyst β-FeOOH/resin, *J. Photochem. Photobiol. A-Chem.*, 2010, 212(2–3): 94-100

24 C. Ruales-Lonfat, J. F. Barona, A. Sienkiewicz, M. Bensimon, J. Velez-Colmenares, N. Benitez, C. Pulgarin, Iron oxides semiconductors are efficients for solar water disinfection: A comparison with photo-Fenton processes at neutral pH, *Appl. Catal. B-Environ.*, 2015, 166: 497-508

25 R. Molina, Y. Segura, F. Martinez, J. A. Melero, Immobilization of active and stable goethite coated-films by a dip-coating process and its application for photo-Fenton systems, *Chem. Eng. J.*, 2012, 203: 212-222

26 W. Y. Huang, M. Brigante, F. Wu, K. Hanna, G. Mailhot, Effect of

ethylenediamine-N,N'-disuccinic acid on Fenton and photo-Fenton processes using goethite as an iron source: optimization of parameters for bisphenol A degradation, *Environ. Sci. Pollut. Res.*, 2013, 20(1): 39-50

27 J. An, L. Zhu, N. Wang, Z. Song, Z. Yang, D. Du, H. Tang, Photo-Fenton like degradation of tetrabromobisphenol A with graphene $BiFeO_3$ composite as a catalyst, *Chem. Eng. J.*, 2013, 219: 225-237

28 H. Qiu, S. J. Zhang, B. C. Pan, W. M. Zhang, L. Lv, Oxalate-promoted dissolution of hydrous ferric oxide immobilized within nanoporous polymers: Effect of ionic strength and visible light irradiation, *Chem. Eng. J.*, 2013, 232: 167-173

29 N. Lu, Y. Lu, F. Y. Liu, K. Zhao, X. Yuan, Y. H. Zhao, Y. Li, H. W. Qin, J. Zhu, $H_3PW_{12}O_{40}/TiO_2$ catalyst-induced photodegradation of bisphenol A (BPA): Kinetics, toxicity and degradation pathways, *Chemosphere*, 2013, 91(9): 1266-1272

30 S. Kakuta, T. Numata, T. Okayama, Shape effects of goethite particles on their photocatalytic activity in the decomposition of acetaldehyde, *Catal. Sci. Technol.*, 2014, 4(1): 164-169

31 R. X. Huang, Z. Q. Fang, X. B. Fang, E. P. Tsang, Ultrasonic Fenton-like catalytic degradation of bisphenol A by ferroferric oxide (Fe_3O_4) nanoparticles prepared from steel pickling waste liquor, *J. Colloid Interface Sci.*, 2014, 436: 258-266

32 G. B. O. de la Plata, O. M. Alfano, A. E. Cassano, Optical properties of goethite catalyst for heterogeneous photo-Fenton reactions - Comparison with a titanium dioxide catalyst, *Chem. Eng. J.*, 2008, 137(2): 396-410

33 M. C. Lu, J. N. Chen, H. H. Huang, Role of goethite dissolution in the oxidation of 2-chlorophenol with hydrogen peroxide, *Chemosphere*, 2002, 46(1): 131-136

34 J. Lusk, B. O. E. Calder, The composition of sphalerite and associated sulfides in reactions of the Cu-Fe-Zn-S, Fe-Zn-S and Cu-Fe-S systems at 1 bar and temperatures between 250 and 535 degrees C, *Chemical Geology*, 2004, 203(3-4): 319-345

35 G. S. Zhang, W. Zhang, D. Minakata, Y. S. Chen, J. Crittenden, P. Wang, The pH effects on H_2 evolution kinetics for visible light water splitting over the $Ru/(CuAg)_{0.15}In_{0.3}Zn_{1.4}S_2$ photocatalyst, *Int. J. Hydrog. Energy*, 2013, 38(27): 11727-11736

36 S. Li, G. Zhang, P. Wang, H. Zheng, Y. Zheng, Microwave-enhanced Mn-Fenton process for the removal of BPA in water, *Chem. Eng. J.*, 2016, 294: 371-379

37 W. Ferraz, L. C. A. Oliveira, R. Dallago, L. d. Conceição, Effect of organic acid to enhance the oxidative power of the fenton-like system: Computational and empirical evidences, *Catal. Commun.*, 2007, 8(2): 131-134

38 J. H. Ma, W. H. Ma, W. J. Song, C. C. Chen, Y. L. Tang, J. C. Zhao, Y. P. Huang, Y. M. Xu, L. Zang, Fenton degradation of organic pollutants in the presence of low-molecular-weight organic acids: Cooperative effect of quinone and visible light, *Environ. Sci. Technol.*, 2006, 40(2): 618-624

39 J. Lee, J. Kim, W. Choi, Oxidation of aquatic pollutants by ferrous–oxalate

complexes under dark aerobic conditions, *J. Hazard. Mater.*, 2014, 274: 79-86
40 C. Madigan, Y. K. Leong, B. C. Ong, Surface and rheological properties of as-received colloidal goethite (alpha-FeOOH) suspensions: pH and polyethylenimine effects, *Int. J. Miner. Process.*, 2009, 93(1): 41-47
41 M. Safiur Rahman, M. Whalen, G. A. Gagnon, Adsorption of dissolved organic matter (DOM) onto the synthetic iron pipe corrosion scales (goethite and magnetite): Effect of pH, *Chem. Eng. J.*, 2013, 234: 149-157
42 Y. Min, K. Zhang, W. Zhao, F. Zheng, Y. Chen, Y. Zhang, Enhanced chemical interaction between TiO_2 and graphene oxide for photocatalytic decolorization of methylene blue, *Chem. Eng. J.*, 2012, 193: 203-210
43 M. E. Lindsey, M. A. Tarr, Inhibition of hydroxyl radical reaction with aromatics by dissolved natural organic matter, *Environ. Sci. Technol.*, 2000, 34(3): 444-449
44 E. M. Rodríguez, G. Fernández, P. M. Álvarez, R. Hernández, F. J. Beltrán, Photocatalytic degradation of organics in water in the presence of iron oxides: Effects of pH and light source, *Appl. Catal. B-Environ.*, 2011, 102(3–4): 572-583
45 J. Lei, C. S. Liu, F. B. Li, X. M. Li, S. G. Zhou, T. X. Liu, M. H. Gu, Q. T. Wu, Photodegradation of orange I in the heterogeneous iron oxide–oxalate complex system under UVA irradiation, *J. Hazard. Mater.*, 2006, 137(2): 1016-1024

Graphical Abstract

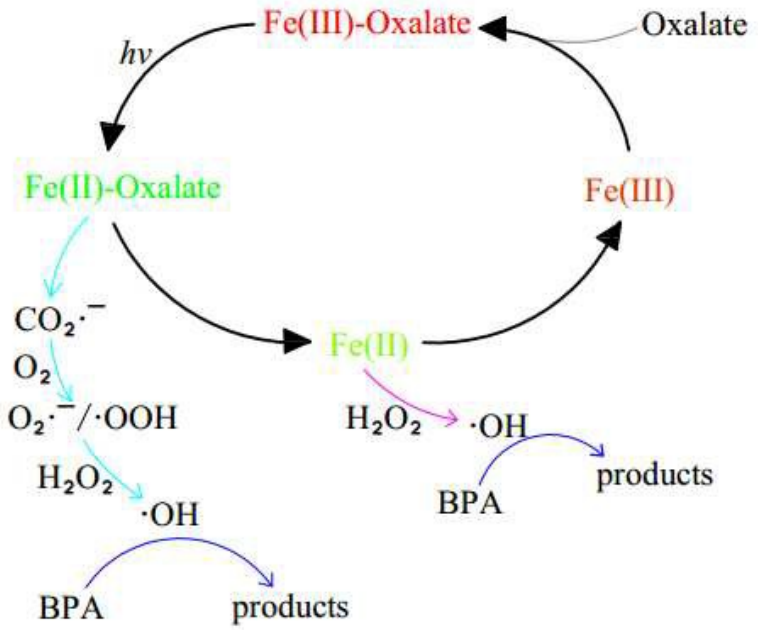

Proposed reaction mechanism of BPA photodegradation in α-FeOOH-oxalate synergistic system.